

Supplemental information

Antibody	Clone	Isotype	Antibody Concentration (µg/ml)		HS578T				MCF7				SKBR3			
			FCM [PE]	SPRi [Unlabeled]	FCM MFI (MESF)		SPRi (RU)		FCM MFI (MESF)		SPRi (RU)		FCM MFI (MESF)		SPRi (RU)	
					Cells	EVs	Cells	EVs	Cells	EVs	Cells	EVs	Cells	EVs	Cells	EVs
CD9	ML13	IgG1	0.63 ²	5 ²	1881	35	247	48	3178	30	398	95	6307	33	298	24
CD44	BJ18	IgG1	5 ¹	5 ¹	851450	698	3730	360	316392	58	1053	348	2018	16	12	-10
CD49e	NKI-SAM-1	IgG2b	10 ¹	5 ¹	70490	147	3563	343	888	69	82	7	2966	16	154	58
CD63	CLB-Gran/12	IgG1	1.5 ⁴	5 ⁵	6086	91	103	-12	1423	38	3	-11	2362	16	34	0
CD71	CY1G4	IgG2a	10 ¹	5 ¹	230471	215	1050	323	32005	73	403	57	309900	29	664	323
CD221	1H7/CD221	IgG1	10 ¹	5 ¹	1491	107	-89	10	5271	30	250	47	3427	16	67	-9
CD227	16A	IgG1	20 ¹	5 ¹	22201	147	265	106	918	38	38	-3	50005	20	240	6
EGFR	AY13	IgG1	10 ¹	5 ¹	55466	131	693	71	11073	77	313	552	18295	20	383	330
EpCAM	VU1D9	IgG1	1.58 ³	5 ⁶	1008	35	317	29.3	259829	337	1199	1323	113213	71	417	95
Her2	Her81	IgG1	10 ⁶	5 ⁶	2771	51	342	-1	9935	19	328	362	381026	113	864	786
Her3	1B4C3	IgG2a	1.25 ¹	5 ¹	661	35	-173	-11	4653	15	316	0	8889	12	271	-10
Blank *			-	-	598	12	78	-37	306	11	-7	-2	546	12	-12	-1
IgG1 *	X40		20 ²	5 ²									2133	25	-42	-22
			10										1052	16		
			5		598	63	392	50					883	16		
			1.5										658	12		
			0.63		755	19		19					630	12		
IgG2a *	X39		10 ²	5 ²	567	27	17	-30	306	19	-13	-9	630	12	-23	-15
			1.25										546	12		
IgG2b *	MG2b-57		10 ¹	5 ¹	661	27	28	4	335	23	-20	-6	658	12	-16	4

Table 1. Results for the antibody panel on both FCM and SPRi. Eleven different antibodies were used, together with corresponding isotype controls and blank control. Used antibody concentrations are shown, together with results for the three different cell lines, on the two techniques, for both cells and EVs.

Manufacturer of antibody:

- ¹ Biolegend, San Diego, CA
² BD Biosciences, San Jose, CA
³ Sigma Aldrich, St. Louis, MO

- ⁴ Beckman Coulter, Fullerton, CA
⁵ Sanquin, Amsterdam, The Netherlands
⁶ Own hybridoma cell line, Enschede, The Netherlands

* Note on EV FCM background signals:

- EV auto-fluorescence
- System noise
- Unbound dye
- Non-specifically bound dye

} **Blank control**
Mean: 12 MESF

} **Isotype control**
Mean: 21 MESF

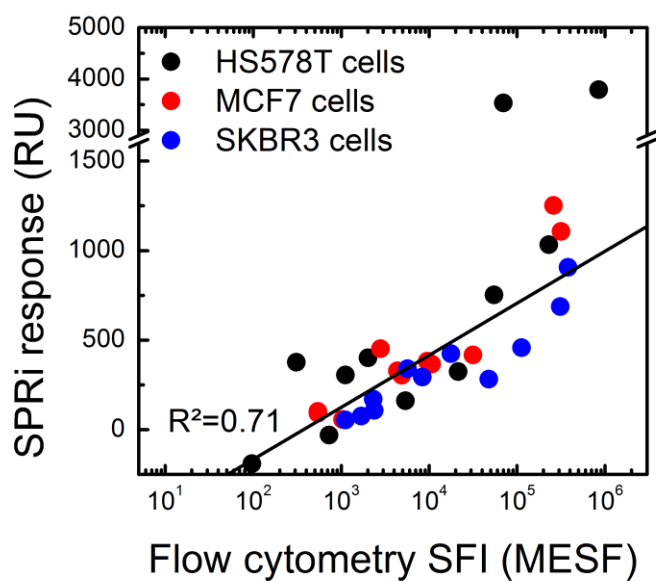


Figure 1. Correlation between antigen detection on SPRi and FCM responses, performed on the combination of cells of three different cell lines. Each cell line was tested with the antibody panel consisting of 11 different antibodies. Two antibodies on HS578T cells were excluded for the correlation. Remaining data shows a correlation between SPRi response and FCM SFI ($R^2=0.71$).

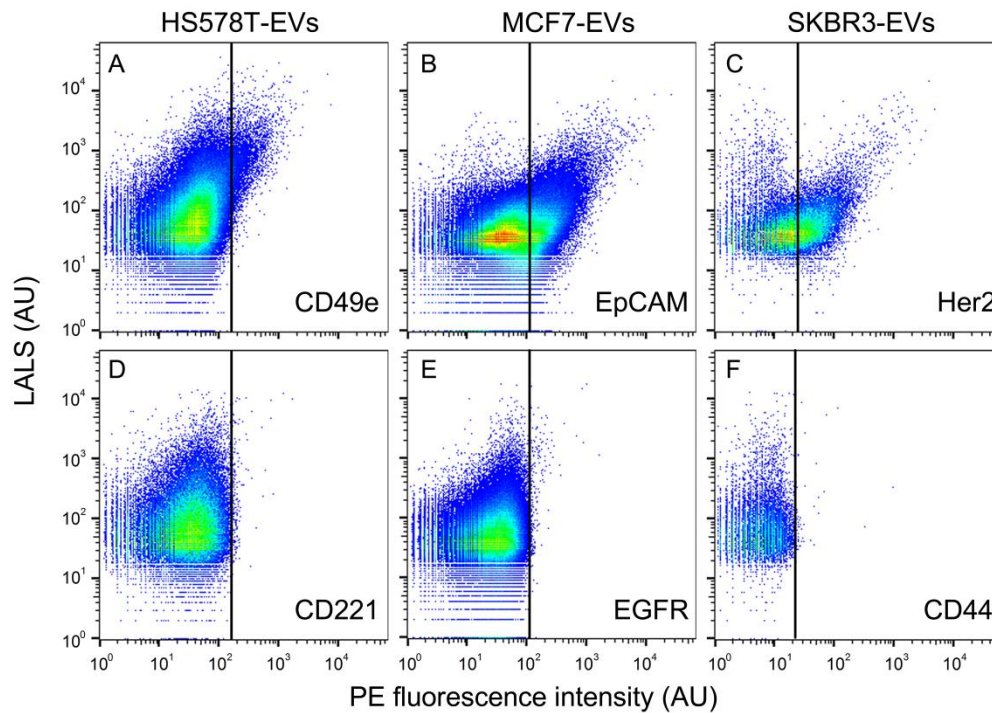


Figure 2. Six example FCM results. Isotype-based gates are added to indicate background levels. The SFI of CD49e, EpCAM and Her2 exceeded the LOD on HS578T-EVs, MCF7-EVs and SKBR3-EVs, respectively. Meanwhile, CD221, EGFR and CD44 did not exceed the LOD. The plots illustrate that positivity is mainly caused by particles with larger scatter intensities. Since the detection limit of our Apogee A50 is approximately 200 nm EV, it is expected that only >200 nm EV contribute to the fluorescence intensities, and that larger particles (>400 nm) have the biggest influence.

EV sample volume in SPRI

SPRI responses are depending on the capture of EVs on the surface. The largest delay in this process is caused by the transport of EVs towards the surface, which is affected by their diffusion speed and the back and forth flow applied during EV incubation. To estimate the effective sample volume that contributes to the EV capture, we made three approximations (Table 2).

Approximation	Diffusion	Back and forth flow
1	-	-
2	√	-
3	√	√

Table 2. Three approximations were made to estimate the effective sample volume in SPRI.

In the following sections, each approximation is explained separately. To summarize, in the three approximations we find effective sample volumes of 125 nL, 7 nL, and 7 to 37 nL, respectively. The long measurement time requirement is not met for the first approximation of 125 nL, and therefore the sample volume is expected to be somewhere between 7 and 37 nL.

Approximation 1

In the first, most simple, approximation both EV diffusion and the impact of back and forth flow are neglected. This approximation assumes therefore that all EVs present in the sample volume above 1 antibody-coated spot are captured by the antibodies on the surface. The sample chamber is 300 μm high and each antibody-coated spot is approximately 830 x 500 μm in size. The resulting effective sample volume for one spot is therefore 125nL. This approximation is reasonable if the average EV diffusion distance in the measurement time is substantially longer than the 300 μm chamber height. Or in other words, assuming the measurement time is sufficiently long.

Approximation 2

The second approximation contains an estimation of the percentage of EVs that can touch the surface due to diffusion limited transport. With the Stokes-Einstein particle diffusion model, a probability density function (P , equation 1) can be derived to determine the change of an EV of diameter d , starting at position x_0 , to diffuse during time t to position x . The temperature T , Boltzmann constant k and dynamic viscosity of water η are known constants. The 1D diffusion constant D is given in equation 2.

$$P(d, x, t) = \frac{1}{\sqrt{4\pi D(d)t}} \exp\left(-\frac{(x-x_0)^2}{4D(d)t}\right) \quad (1)$$

$$D(d) = \frac{kT}{3\pi\eta d} \quad (2)$$

An example is shown in Fig. 3 of the resulting probability density function for different EV diameters (panel A) and different incubation times (panel B).

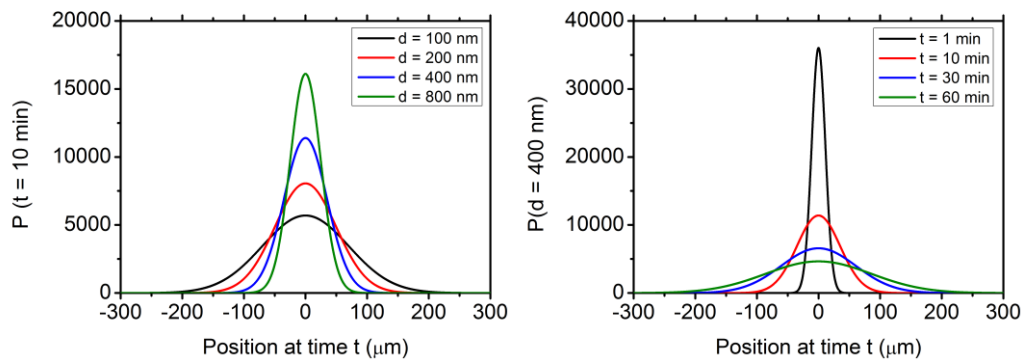


Figure 3. Probability density function for 1D diffusion of different particle diameters (left) and different incubation times (right). *Smaller particles diffuse faster and therefore have a wider distribution in the left graph after 10 minutes. This distribution spreads out further at longer measurement times, as shown by the right graph.*

The area under the probability density function represents the chance that an EV starting at one position (x_0) ends up in another (x) after time t . Therefore it can be used to calculate the chance that an EV starting at a distance x from the surface will diffuse ‘through’ the surface. Because the outcome of the probability density function represents the chance of an individual EV to end up at the surface, it directly can be translated to the percentage of all EVs originating from height x , with diameter d , that diffuse ‘through’ the surface within time t . The absolute number of EVs was derived from this percentage by defining the measurement time of 600 s, integrating over $x=[0,300 \mu\text{m}]$ and multiplying it with the EV particle size distribution and the spot surface area. To find the effective sample volume, we divided this number of captured EVs by the total EV concentration of the sample and multiplied it with the total 125 nL of volume above the spot (see approximation 1).

The resulting effective sample volume is 7 nL, indicating that only a fraction of all EVs above the spot has the possibility to touch the surface (6%). Furthermore, the captured EVs are on average smaller than the average EV size in the starting material due to the faster diffusion of small EVs.

The Stokes-Einstein particle diffusion model is a basic model for the motion of ‘sparse’ particles in suspension. We did not consider any models encompassing particle-particle interactions because the particle density of the EV preparations is in the order of 0.01% (v/v).

Approximation 3

In the third approximation, we added the maximum potential increase in number of captured EVs compared to approximation 2 due to the application of back and forth flow. Back and forth flow is basically a two-step pump action, in which firstly extra sample is injected and secondly the same amount of sample back is taken back. Therefore the sample in the sample chamber flows forward in the first half of the cycle and backwards in the second half of the cycle and more EVs are able to touch the spot. The back and forth flow is parallel to the sensor surface, with a Reynolds number of approximately 1. Therefore there is no turbulence in the flow chamber, which indicates that the back and forth flow does not directly affect the transport of EVs to the surface.

However, according to the manufacturer, the number of captured EVs is enhanced due to back and forth flow. The total sample volume above the spot is increased 9 times with the injection of 14 mL in the entire sample chamber. However, due to the laminar flow profile and no-flow boundary conditions, the largest sample displacement is in the middle of the chamber (Fig. 4A). Therefore it affects EVs of different diameters differently, as small EVs captured on the surface can diffuse larger distances than large EVs. An estimation is made of the additional availability of EVs due to the back and forth flow by taking a power law fit of the EV size distribution into account (Fig. 4B), and the results from approximation 2.

It was found that the effective sample volume increased from 7 nL to approximately 37 nL with the application of back and forth flow. This is, however, an overestimation of the effective sample volume since EVs could diffuse to regions on the surface which are outside the capture spot. The effective sample volume with back and forth flow is somewhere between the 37 nL and the 7 nL, which was estimated in the no-flow approximation.

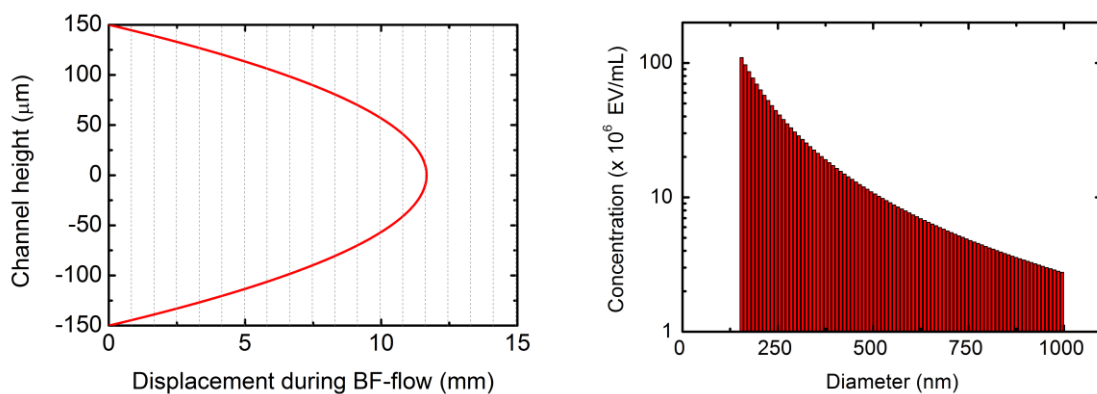


Figure 4. Left: Sample displacement profile during back and forth flow. Right: Power law fit of the SKBR3-EVs size distribution used in the SPRI measurements with the EV concentration range.